Materials Science & Engineering A 683 (2017) 129–134

Contents lists available at ScienceDirect

Materials Science & Engineering A

journal homepage: www.elsevier.com/locate/msea

Effect of grain boundary on the precipitation behavior and hardness of Al-Cu-Mg alloy bicrystals during stress-aging

Xiaobin Guo[a], Yunlai Deng[a,b,*], Jin Zhang[b,c], Xinming Zhang[a,b]

[a] School of Materials Science and Engineering, Central South University, Changsha, China
[b] State Key Laboratory of High Performance and Complex Manufacturing, Central South University, Changsha, China
[c] Light Alloy Research Institute, Central South University, Changsha, China

ARTICLE INFO

Keywords:
Al-Cu-Mg alloys
Bicrystal
Crystallographic orientation
Precipitation
Grain boundary
Stress-aging

ABSTRACT

While it is clear that precipitates near grain boundaries in aluminum alloys nucleate more easily and grow more quickly, the mechanism of how the grain boundaries influence the anisotropic distribution of *S* precipitates is still unknown. In this study, a bicrystal Al-Cu-Mg alloy specimen was prepared to obtain a single grain boundary. The precipitation distribution and hardness of the Al-Cu-Mg alloy bicrystal were analyzed after stress aging at 30 MPa. Transmission electron microscopy was used to analyze the precipitation behavior of *S* precipitates, and the hardness was tested along the location on the bicrystal specimen. The hardness of the right area around the grain boundary is lower than that of the left area around the grain boundary after stress aging. The precipitation behavior around the grain boundary is different from that in the matrix. For the left area near the grain boundary with the $(1, -1, 8)_{Al}$ plane orientation, the anisotropic distribution of the *S* precipitates is inhibited. For the right area near the grain boundary with the $(3, 5, 6)_{Al}$ plane orientation, the anisotropic distribution of the *S* precipitates is even more pronounced than that in the right matrix. This difference in the influence depends on the crystallographic orientations of the matrix around the two sides of the grain boundary.

1. Introduction

An inhomogeneous distribution of precipitates is induced in the aluminum matrix when alloys are aged under applied stress [1–10]. As observed from the transmission electron microscopy (TEM) images, stresses induce precipitates to distribute more in some $<100>_S$ directions and less in others. An anisotropic distribution of the precipitates leads to anisotropy of the mechanical properties of aluminum alloys [8,9]. *S* precipitate is the main phase in the Al-Cu-Mg series alloys and always forms in the face-centered orthorhombic structure on the $\{012\}_{Al}$ habit planes and grows along the $<001>_{Al}$ directions [15]. Previous investigation [10] of the Al-Cu-Mg alloys aged under elevated compression stresses indicated that for aging under a lower stress, an obviously anisotropic *S* precipitate distribution is present, and the mechanical properties were degraded. Conversely, at higher applied stress such as 50 MPa, *S* precipitates dispersed more homogeneously due to the influence of dislocations.

In the manufacturing process, Al-Cu-Mg alloys are always polycrystalline with a large amount of grain boundaries [2]. Along the grain boundaries, the atoms are located in a disordered arrangement and lack regular bonding. The extra energy near the grain boundary makes the diffusion of the solute atoms more active [11–14]. With the exception of the inhibiting effect of the dislocations [10], the effect of the grain boundaries in polycrystalline alloys cannot be neglected. Due to the difficulty in selecting a single grain boundary with a known orientation from the polycrystalline specimen, the mechanism of how the grain boundaries influence the anisotropic distribution of *S* precipitates is still unknown.

In this study, an Al-Cu-Mg alloy bicrystal specimen was prepared to obtain a single grain boundary. The effect of the grain boundary on the precipitation behavior and hardness of the alloys during stress aging was studied. Contrary to the current understanding that grain boundaries always promote precipitation and induce an inhomogeneous distribution, we found that the effect depends on the crystallographic orientations of the matrix on the two sides around the grain boundary.

2. Experimental procedures

The chemical composition of the Al-Cu-Mg alloy in this work is given in Table 1. An Al-Cu-Mg alloy plate with a thickness of 8 mm was used to prepare the bicrystal specimen. The bars cut from the plate were pulled to 0.5–1.0% strain, followed by annealing at 525 °C for

* Corresponding author at: School of Materials Science and Engineering, Central South University, Changsha, China.
E-mail address: luckdeng@csu.edu.cn (Y. Deng).

http://dx.doi.org/10.1016/j.msea.2016.12.002
Received 9 November 2016; Accepted 1 December 2016
Available online 01 December 2016
0921-5093/

Table 1
Composition of Al-1.23Cu-0.43Mg alloy in weight percent.

Alloys	Cu	Mg	Si	Fe	Zn	Al
Al-Cu-Mg	1.23	0.43	0.02	0.03	0.01	Balance

24 h, and the strain-annealing cycle was repeated 8–10 times. Finally, bar specimens with macro-grains up to 10 mm in diameter were prepared. The bicrystal specimen was cut from the macro-grains bars using a spark-erosion cutting machine. The optical micrograph of the Al-1.23Cu-0.43Mg alloy bicrystal is shown in Fig. 1(a).

The orientation of the bicrystal specimen was determined by electron backscatter diffraction (EBSD) in the Helios Nanolab™ 600i using a Field Emission Gun LEO 1530 operated at 20 kV. Prior to the examination, the bicrystal samples were electrolytically polished using 10% perchloric acid+90% ethanol at 21 V and −15 °C. The mapping and orientation analysis of the bicrystal were performed using the OIM Analysis 6.0 software, with the Inverse Pole Figure (IPF) shown in Fig. 1(b). The plane orientation of the left matrix in the bicrystal is $(1, -1, 8)_{Al}$, while that of the right matrix is $(3, 5, 6)_{Al}$. The rotation axis of the grain boundary is [16, −7, −6], and the rotation angle is 44.6°.

The bicrystal specimen was sliced into two parts, and both parts were first solution treated at 525 °C for 2 h then quenched with water. The aging of the two specimen parts was performed at 180 °C for 66 h, with one part under conventional free-stress conditions and another under an applied compressive stress of 30 MPa. The stress was applied perpendicular to the plane orientation of the bicrystal samples.

Transmission electron microscopy (TEM) foils were examined using a Titan G2 60-300 with an image corrector microscope operated at 300 kV. The sampling location of three areas in the bicrystal is shown in Fig. 2. For the two sides of the matrix of the bicrystal, Sample 1 is on the left with the $(1, -1, 8)_{Al}$ plane orientation, and Sample 2 is on the right with the $(3, 5, 6)_{Al}$ plane orientation; disks with a diameter of 3 mm were punched from the aged samples, ground to a thickness of ~0.1 mm, and then twin-jet electro polished in a solution of 25% nitric acid +75% methanol at 20 V and −25 °C. To accurately detect the grain boundary, TEM foils near the grain boundary (Sample 3) were prepared by focused ion beam (FIB) techniques in the Helios Nanolab™ 600i using a Ga ion beam. The Vickers hardness of the aged specimen was measured in a Huayin® HV-5 micro-hardness tester.

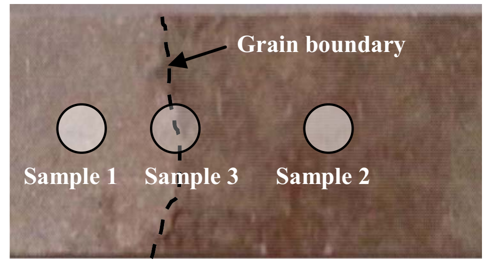

Fig. 2. Sampling location and sample numbers of three types of TEM foils.

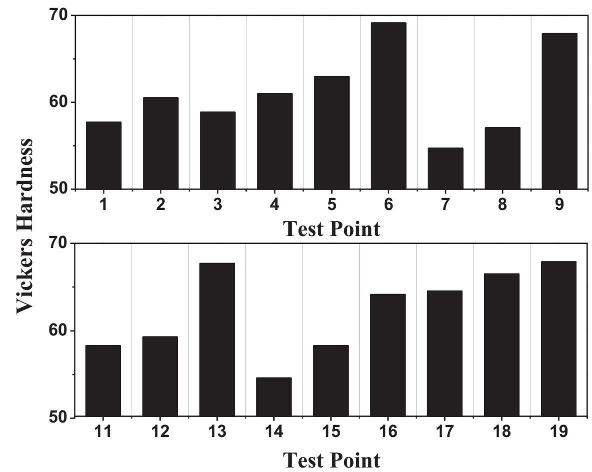

Fig. 3. Hardness results along the location on Al-1.23Cu-0.43Mg alloy bicrystal specimen after aging at 180 °C for 66 h under 30 MPa of applied stress.

3. Results

3.1. Hardness in stress-aged Al-Cu alloy bicrystal

The hardness results of the Al-1.23Cu-0.43Mg alloy bicrystal obtained after stress-aging at 180 °C for 66 h under 30 MPa are shown in Fig. 3. To study the change in the hardness along the location on the bicrystal, the hardness was tested along two lines. Twenty hardness points were chosen, with one part sampled by points 1–9 and another by points 11–19; points 6, 7, 13 and 14 were tested near the grain boundary, as shown in Fig. 4a. The hardness test direction and crystallographic orientation of the bicrystal specimen are also shown in Fig. 4b.

With different plane orientations, the hardness values of the two sides of the matrix in the bicrystal remain distinct. The effect of the grain boundary on the hardness of the stress-aged bicrystal is apparent in Fig. 3a and b; the hardness values at points 6 and 13 are higher than the values in the matrix, but the values at points 7 and 14 are lower.

3.2. Precipitation behavior of S-plates in bicrystal

TEM images were observed from the $<112>_{Al}$ axis, and three *S* precipitate variants $[100]_S$, $[010]_S$ and $[001]_S$ could be seen, as shown by the white arrows in Figs. 5 and 6. TEM images of Sample 1 in the left matrix, Sample 2 in the right matrix, and Sample 3 on the grain boundary were observed in the bicrystal after free-stress aging (as shown in Fig. 5) and stress aging at 30 MPa (as shown in Fig. 6). Sample 3 has been tilted twice in TEM in order to observe the *S* precipitates' behavior in two orientation planes around the grain boundary, and therefore, the TEM images of Sample 3 were shown from the left and right of the grain boundary.

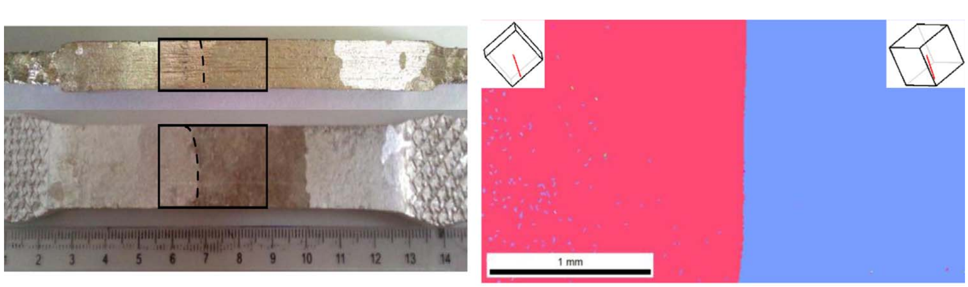

(a) (b)

Fig. 1. Macrograph (a) and orientation map (b) of Al−1.23Cu−0.43Mg alloy bicrystal specimen.